

JAAS

Accepted Manuscript



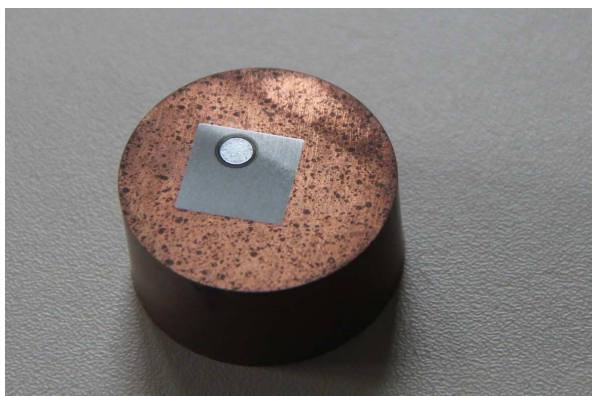
This is an *Accepted Manuscript*, which has been through the Royal Society of Chemistry peer review process and has been accepted for publication.

Accepted Manuscripts are published online shortly after acceptance, before technical editing, formatting and proof reading. Using this free service, authors can make their results available to the community, in citable form, before we publish the edited article. We will replace this *Accepted Manuscript* with the edited and formatted *Advance Article* as soon as it is available.

You can find more information about *Accepted Manuscripts* in the [Information for Authors](#).

Please note that technical editing may introduce minor changes to the text and/or graphics, which may alter content. The journal's standard [Terms & Conditions](#) and the [Ethical guidelines](#) still apply. In no event shall the Royal Society of Chemistry be held responsible for any errors or omissions in this *Accepted Manuscript* or any consequences arising from the use of any information it contains.

1
2
3 Table of contents entry:
4
5
6
7
8
9
10
11
12
13
14
15
16
17
18
19
20



21 Excitation and ionization processes of iron ions in argon-, neon- and argon-hydrogen glow
22 discharges are described based on transition rate diagrams.
23
24
25
26
27
28
29
30
31
32
33
34
35
36
37
38
39
40
41
42
43
44
45
46
47
48
49
50
51
52
53
54
55
56
57
58
59
60

Excitation and transition rate diagrams of singly ionized iron in analytical glow discharges in argon, neon and argon-hydrogen mixture

Zdeněk Weiss^a, Edward B.M. Steers^b, Juliet C. Pickering^c and Sohail Mushtaq^b

Receipt/Acceptance Data [DO NOT ALTER/DELETE THIS TEXT]

Publication data [DO NOT ALTER/DELETE THIS TEXT]

DOI: 10.1039/b000000x [DO NOT ALTER/DELETE THIS TEXT]

Abstract

The emission spectra of iron observed using a Grimm-type glow discharge in argon, argon with 0.3% v/v hydrogen and neon were studied to identify major excitation and ionization processes of iron ions in the plasma. Transition rate diagrams are given for iron ions in those discharges. These are particularly useful for describing situations in which the rate of radiative decay of excited states is comparable to or exceeds the rate of their collisional de-excitation. Relations between transition rate diagrams and Boltzmann plots are discussed. The following processes were identified to be responsible for excitation of Fe II glow discharge spectra: charge transfer from argon/neon ions to ground state- and metastable iron atoms, Penning excitation of ground state- and metastable iron ions by argon metastables and collisional excitation by electrons of metastable iron ions. No evidence was found that local thermodynamic equilibrium exists for iron ions in a glow discharge plasma in any interval of excitation energies. Open questions remain concerning charge transfer excitation of iron, in particular about the range of energies in which the Fe II levels can be directly populated by charge transfer and about conservation of spin in such reactions.

1. Introduction

Emission spectra produced by analytical glow discharges^{1,2} differ significantly from spectra generated by other common sources, such as ICP, spark, arc and laser-induced plasmas, reflecting different mechanisms that dominate the excitation and ionization of the analyzed elements³⁻⁵. The demand for a better understanding of excitation processes in analytical glow discharges has increased during the past decade after the introduction of CCD spectrometers that can measure emission spectra over wide continuous wavelength ranges, giving a large number of observed lines for most elements. To decide which lines are suitable for analysis of a given element in a given analytical application and to treat properly various excitation-related matrix effects⁶ are other reasons for the continuing work in this area.

There are two common methods that have been used in those studies so far: the first method is based on ratios of intensities of observed lines in a certain experiment and in another experiment with changed discharge conditions. The plot of these ratios as a function of excitation energy then reflects populations of different excited levels at the changed conditions relative to the populations at the 'reference' conditions, and is suitable to identify prospective selective excitation processes. This approach has been successfully used in glow discharge optical emission spectrometry (GD-OES) over

the past ca 30 years and led to great progress in understanding the role of selective excitation processes in analytical glow discharges⁷⁻⁹ and also e.g. in ICP¹⁰. An advantage of using intensity ratios is that they are independent of the sensitivity function of the instrument used. However this approach has some serious drawbacks, e.g. that intensity ratios cannot be established for lines that do not exist (are not observed) in one of the two experiments, comparison of which is under study. The second most common approach assumes that the populations of various excited levels of an atom or ion under study reflect some kind of equilibrium maintained by collisions between those atoms and ions and other species in the plasma and investigates whether or to which extent the observed intensities reflect the Boltzmann distribution of those populations (the Boltzmann plot)¹¹⁻¹³.

Recently, a new formalism was proposed by Weiss et al.¹⁴ to describe systematically radiative transitions occurring in emission spectra of an element and draw conclusions about the excitation processes involved. In this formalism, the rates of observed radiative transitions are evaluated and then plotted as functions of energy of the levels involved. Such plots are called transition rate diagrams (TR diagrams). These diagrams can yield more complete information about the observed spectra than either of the two methods mentioned above and do not depend on any assumptions about the actual population distributions, such as assumptions utilizing the concept of the local thermodynamic equilibrium (LTE). This was demonstrated on the spectra of neutral and singly ionized manganese emitted by a Grimm-type glow discharge in argon, neon and an argon-hydrogen mixture¹⁴. To determine a TR diagram, the sensitivity function of the instrument used must be known and it is

^a LECO Instrumente Plzeň, spol. s r.o., Plaská 66, 323 25 Plzeň, Czech Republic.; E-mail: weissz@leco.cz

^b London Metropolitan University, 166-220 Holloway Road, London, N7 8DB, UK

^c Blackett Laboratory, Imperial College London, Prince Consort Road, London, SW7 2AZ, UK

necessary to consider all observable lines, not only a narrow wavelength region. These conditions apply to the Boltzmann plots as well. The successful application of TR diagrams for manganese suggests the use of this approach also for other elements and this study is an attempt to do so for the glow discharge spectra of singly ionized iron. Besides its importance in analytical applications, iron was selected also because its electron structure is well known and a reliable classification of Fe II emission lines can be found in the literature.

The excitation of iron in glow discharges has been studied extensively in various experimental setups and under differing conditions^{8,9,11-13,15-22}. This paper is an attempt to describe major excitation processes of ionized iron in analytical glow discharges as completely as possible, based on the formalism of TR diagrams. Besides argon, which is the most common discharge gas in analytical applications, results for a discharge in neon are also included, to compare with an argon discharge and because discharges in neon may be useful in some situations. For a proper selection of analytical lines and interpretation of analytical data, it is often important to consider effects on emission spectra of hydrogen and other reactive gases, which may be present as impurities in the discharge gas or may come from the sample^{18, 19}. Therefore, results for a glow discharge in argon with a small addition of hydrogen are also described.

Iron is a transition element with a complex atomic structure that results from the partly filled 3d subshell. Fig. 1 gives schematic diagrams of the term structure of Fe II. The ground state term of the Fe ion is a sextet, $3d^6(^5D)4s\ a^6D$. The term structure of Fe II is formed by $3d^5\ nln'l'$, $3d^6\ nl$ and $3d^7$ systems. The singly excited ('normal') system is built on the $3d^6(^M L)\ nl$ set of configurations, where (^ML) is the associated parent term in Fe III, and *nl* is the valence electron that defines the orbital. In the term diagram the configurations are arranged according to their parent terms. Only the orbital configurations are labelled. The boxes represent the energy range of all the known levels in a given subconfiguration. The doubly excited system, $3d^5(^M L)\ nln'l'$, is built upon the grandparent terms $3d^5(^M L)$ in Fe IV. Many intermediate and high-lying levels in both the normal and doubly excited systems are affected by configuration mixing, giving more observed transitions than would be expected if LS selection rules were fully obeyed. A detailed description of the state of knowledge of the Fe II energy level system and spectrum can be found in Johansson²⁰ and Nave & Johansson²¹, where many newly identified lines and energy levels are reported.

2. Transition rate diagrams

The energy of a photon emitted in transition from level *i* to level *j* is $E_{ij} = E_i - E_j = hc/\lambda_{ij}$. The intensity of the spectral line is that energy multiplied by the number of

transitions per second, n_{ij} , namely $I_{ij} = n_{ij}hc/\lambda_{ij}$. Hence the transition rate $n_{ij} = I_{ij}\lambda_{ij}/hc$ is proportional to the product $I_{ij}\lambda_{ij}$ of the intensity I_{ij} of the emission line associated with the transition $i \rightarrow j$ and its wavelength λ_{ij} . Transition rates associated with different emission lines can then be evaluated from the observed spectrum, except for a common multiplicative constant. In this sense, the quantities referred to as transition rates are transition rates expressed in some arbitrary units that are the same throughout the whole paper. In these considerations, it is supposed that the variations of instrument sensitivity with wavelength are known and corrected for, so that the "intensities" are on a uniform scale throughout. Every emission line in the spectrum starts at a certain excited level *i* and ends at a level *j*. Hence, level *i* is radiatively *depopulated* by the transition associated with this line and the level *j* is radiatively *populated* by that transition. Thus each level *i* is radiatively depopulated at a rate equal to the sum of the rates of all transitions associated with the lines of which *i* is the upper level. Similarly, a level is radiatively populated at a rate equal to the sum of the rates of the radiative transitions populating this level, i.e., those transitions for which it is the lower level. As an example, this calculation is shown in Table 1 for the level $3d^6(^5D)4p\ z^6P^{\circ}_{3/2}$ of Fe II in a glow discharge in neon. In the upper part of the table, 10 transitions are listed, which populate this level by decay of higher excited states (cascade excitation), and in the lower part of the table 4 transitions which depopulate this level are listed. The rate of each transition (column 7) was calculated as the product $I_{ij}\lambda_{ij}$ of the intensity I_{ij} of the corresponding line and its wavelength λ_{ij} . Total excitation/de-excitation rates of this level are given in the final column. Because the de-excitation rate of this level is ca 1.8 times higher than the rate of its cascade excitation, an additional excitation of this level by collisional processes must occur, because, under steady conditions of the discharge, excitation and de-excitation rates of each level must be equal. Total radiative excitation/de-excitation rates of different levels are then plotted as a function of their energy, where the de-excitation rates are represented by blue points as positive values, and the rates of radiative excitation by transitions from higher levels are represented by red points with values increasing downward, see Fig. 2. The resulting plot is called the TR diagram¹⁴. TR diagrams are particularly useful for studying excitation processes in low pressure plasmas such as glow discharges, in which lifetimes of most excited states are largely limited by radiative decay. In such situations, the rate of collisional excitation of a given state is equal to the difference between the rate of its radiative de-excitation and the rate of its radiative excitation, which can both be calculated from the emission spectrum. It should be noted that the formalism of TR diagrams, as presented above, gives an accurate picture only if the self-absorption of radiation can be neglected. Otherwise the true rates of radiative de-excitation would be higher

1
2 than their estimates based on the measured line
3 intensities.

4 The ordinate scale in all TR diagrams in this paper is
5 such that (relative) transition rates concern a certain
6 amount of iron sputtered per second, i.e., all transition
7 rates throughout this paper are corrected for different
8 sputtering rates in different discharge gases. Using the
9 terminology common in analytical glow discharge
10 spectroscopy, emission yields are used throughout this
11 paper instead of raw intensities to calculate the rates of
12 radiative transitions²³. Therefore, the TR diagrams for
13 argon-, argon-hydrogen and neon discharges in this
14 paper can be compared on a quantitative basis.

17 3. Experimental details

18
19 The detailed analysis of the observed Fe spectra
20 presented below is based on data from the vacuum-uv
21 high resolution Fourier transform spectrometer (FTS)²⁴
22 at Imperial College London, used in conjunction with a
23 free-standing Grimm-type source¹. Three wavelength
24 ranges were selected by choosing appropriate free
25 spectral ranges and suitable photomultiplier tube
26 detectors and, where needed, optical filters. The
27 combined wavelength range of these FTS measurements
28 was from 151 to 630 nm. The resolution used was:
29 0.035 cm⁻¹ for the visible region (>365 nm); 0.05 cm⁻¹
30 for the intermediate region (250-365 nm), and 0.07 cm⁻¹
31 for the uv-vuv region (151 - 250 nm). This corresponds
32 to a resolution of 0.14 pm at 200 nm. In another set of
33 experiments, the wavelength range was extended up to
34 900 nm (not in a neon discharge). To obtain accurate
35 relative line intensities, the areas under the line profiles
36 were integrated. Calculation of transition rates
37 mentioned above in §2 assumes that the intensities I_{ij}
38 are 'true' intensities, corrected for sensitivity variations
39 of the spectrometer used over the recorded spectral
40 range. Hence, radiometric calibration of the instrument,
41 providing its sensitivity as function of the wavelength,
42 was necessary to obtain the corrected relative
43 intensities. Radiometric calibration was performed using
44 standard lamps, a tungsten-halogen lamp and a
45 deuterium lamp, with known radiation characteristics²⁵,
46 and by the branching ratio method²⁵. If a level has decay
47 channels to more than one lower level, the decay is said
48 to be 'branched'. The ratio $I_{ij}/I_{ij'}$ of intensities of
49 radiation emitted in transitions from the same upper
50 level i to lower levels j and j' is called the branching
51 ratio and is given by the ratio of the corresponding
52 transition probabilities divided by the wavelengths of
53 those lines, $\lambda_{ij}A_{ij}/(\lambda_{ij'}A_{ij'})$, see Ref.²⁵. By comparison of
54 accurately established branching ratios with the actually
55 measured intensity ratios, it is possible to calculate the
56 ratios of the instrument sensitivities at the
57 corresponding wavelengths. In this work, branching
58 ratios in the Fe I²⁶⁻²⁸ and Fe II^{28,29} spectra were used to
59 verify and complement the calibration data obtained
60 using the standard lamps. The procedure will be

described in more detail in a forthcoming paper on a
new catalogue of glow discharge spectra. Work on the
catalogue started some time ago³⁰ in the framework of
the Analytical Glow Discharge Network
"GLADNET"³¹, a Marie Curie Research Training
Network (RTN) funded by the EC under its Sixth
Framework Programme (FP6). The results presented
here are based on the Fe glow discharge spectrum to be
published in this catalogue. Also, some software tools
developed for the catalogue data were successfully used
in this work. 1654 Fe II lines were identified in the
spectrum (638 in an argon discharge and 1501 in a neon
discharge) and 519 levels were considered to construct
the TR diagrams. Classification of the lines is based on
the NIST database²⁸ and the work by Nave and
Johansson²¹. Excitation energies in the Fe II spectrum
are given relative to the ground state of the Fe *atom*
throughout this paper. They differ from excitation
energies relative to the ground state of the Fe⁺ ion, more
usually listed in the tables, by ionization energy of iron,
 $E_i = 7.9024$ eV.

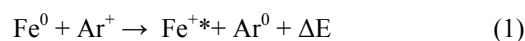
In addition to the FTS measurements, some
complementary data were collected using the LECO
GDS500A GD-OES spectrometer³², a grating instrument
with CCD detection, resolution of 60–70 pm and
wavelength range of 165–465 nm, in the LECO
European Technical Centre, Prague. These data were
particularly useful in investigations of the effects of a
small addition of hydrogen to the argon discharge gas
on the Fe II spectra, described in § 4.3. in this paper, in
the vacuum ultraviolet wavelength region below 200
nm.

All the experiments were carried out with 'standard'
operating conditions of the glow discharge, i.e. a dc
discharge with a 4 mm internal diameter anode, with
constant voltage – constant current stabilization at 700
V, 20 mA. The spectra of iron were collected using a
99.9% pure Fe sample. The discharge gas was argon,
neon or argon with added hydrogen at the level of 0.3%
v/v, below referred to as an Ar(H) mixture. The pressure
of the working gas at the discharge conditions
mentioned above was 5.6 torr for a discharge in argon
and 12.7 torr for a discharge in neon.

295 4. Results and discussion

4.1. Fe II spectrum in argon discharge

TR diagram of Fe II in an argon discharge is shown in
Fig. 2. The most prominent peak in the upper side of the
diagram at ≈ 15.6 eV corresponds to de-excitation of the
Fe II levels populated by asymmetric charge transfer
(ACT) reaction between neutral iron atoms and argon
ions, see e.g. Ref.⁸ by Steers et al.:



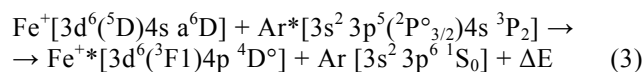
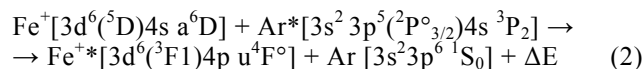
ACT is a resonant process, selectively populating Fe II levels that are close to the energy of Ar ions (15.76 eV and 15.94 eV for the metastable $\text{Ar}^{+*} \text{}^2\text{P}_{1/2}$ ion), so that ΔE is a small positive or negative value. Also, preservation of total spin of the reacting species is assumed for an ACT reaction⁸. This leads to excitation of Fe II quartets and sextets because the ground state term of the Fe atom is a quintet. The most strongly excited Fe II levels by Ar^+ -ACT are those belonging to a sextet term, $3d^5(^6\text{S})4s4p(^3\text{P}) \text{}^6\text{P}^\circ$, (15.59-15.61 eV). Their radiative decay dominates the TR diagram in Fig. 2, populating levels belonging to the Fe II ground term (the $\text{}^6\text{P}^\circ$ - $\text{}^6\text{D}$ multiplet, $\lambda = 161$ -163 nm, marked in the TR diagram in Fig 2) and also levels of the $3d^54s^2 \text{}^6\text{S}$ term at ≈ 10.79 eV ($\text{}^6\text{P}^\circ$ - $\text{}^6\text{S}$, $\lambda = 257$ -258 nm). Close to the sextet term are quartet terms with strong transitions between the levels at 15.50-15.55 eV and 10.53-10.75 eV, $\lambda = 249$ -255 nm. However, the TR diagram in Fig. 2 gives only a very rough outline of the situation and a more detailed view can be obtained by plotting the transition rates on a logarithmic scale and by distinguishing the multiplicities of the levels by different colours of the corresponding points. Such a modified TR diagram is in Fig. 3.

In the Fe II spectrum in an argon discharge, not many levels are subject to cascade processes (excitation by decay of higher excited levels followed by radiative de-excitation) and for those that are, the observed rates of cascade excitation are small compared to their de-excitation rates. Hence, it is very likely that, for most levels, the de-excitation rates in the upper part of the TR diagram in Fig. 3 reflect well their collisional excitation. Concerning the charge transfer reaction mentioned above, levels of the sextet term $3d^5(^6\text{S})4s4p(^3\text{P}) \text{}^6\text{P}^\circ$ are more strongly excited than the nearby quartet Fe II levels with a similar energy: their de-excitation rates are higher by an order of magnitude. A stronger excitation of the sextet levels mentioned above than the nearby quartet levels was observed also by Zhang et al.¹³. If this behaviour is related to the term multiplicity (there are no other Fe II sextet terms with energy suitable for Ar^+ -ACT), it means that parallel orientation of the spins of the reacting particles is preferred over the anti-parallel. Some quartet levels just above the argon ionization energy are also excited, with the excitation rates falling off as the energy difference increases. An expanded portion of the TR diagram between 15 eV and 19 eV is in Fig. 4. It shows that also some *doublet* Fe II levels with energies close to the argon ionization energy are excited. It is unclear how these are excited, as the total spin would not be preserved if they were excited by Ar^+ -ACT. Further discussion of Fe II levels excited by Ar^+ -ACT is in §4.4. below, in comparison with a neon discharge.

The two octet levels at ≈ 14.4 eV in Fig. 3 with low de-excitation rates belong to the term $3d^5(^6\text{S})4s4p(^3\text{P}^\circ) \text{}^8\text{P}^\circ$, are partly metastable and decay by inter-combination transitions to the levels of the ground state

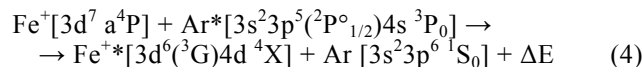
Fe II term, $3d^6(^5\text{D})4s \text{}^6\text{D}$ (a sextet). Therefore, the corresponding transition probabilities are probably low and the populations of these levels are most likely controlled by collisional processes (the positions of the corresponding points in the TR diagram in Fig. 3 do not reflect the rate of their collisional excitation).

From the diagram in Fig. 3, it is apparent that there are also excited levels with relatively high energies, although these are much less excited than levels with energies close to 15.6 eV and lower, and there is a clear trend showing decrease of (collisional) excitation rates with increasing energy. Exceptions to this rule are two well pronounced peaks at ≈ 19.48 eV and ≈ 21.35 eV. The first of these consists of transitions involving two quartet terms, $3d^6(^3\text{F}1)4p \text{}^4\text{F}^\circ$ and $3d^6(^3\text{F}1)4p \text{}^4\text{D}^\circ$, at 19.47-19.49 eV, and most likely reflects the Penning excitation of Fe^+ ground state ions by Ar metastables (E ≈ 11.55 eV):



These reactions have a resonant character and exhibit a perfect energy match, with $\Delta E = 0.02$ - 0.03 eV. Also spin is conserved.

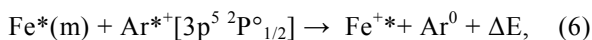
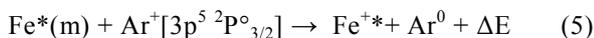
The peak at ≈ 21.35 eV in the TR diagram in Fig. 3 consists of transitions involving the ^4D , ^4G , ^4H , ^4I terms, all with the same subconfiguration, $3d^6(^3\text{G})4d$. In a search for possible energy resonances, it was found that these levels can be excited by Penning excitation of Fe^+ metastables with energies of 9.57-9.63 eV ($3d^7 \text{}^4\text{P}$) in collisions with argon metastables with energy 11.72 eV, $3s^2 3p^5(^2\text{P}^\circ_{1/2})4s \text{}^3\text{P}_0$:



where ^4X means one of the ^4D , ^4G , ^4H , ^4I terms. The $3d^7 \text{}^4\text{P}$ metastable levels of Fe^+ are (weakly) populated by radiative de-excitation of several higher Fe^+ levels, with total cascade excitation rate of the $3d^7 \text{}^4\text{P}$ term of $\approx 2.7 \times 10^3$ units (see the three quartet levels at ca 9.6 eV in the bottom part of the TR diagram in Fig. 3). This would be sufficient to balance the loss of these metastables by the Penning reaction (4) mentioned above, as the combined de-excitation rate of the Fe^+ levels at ≈ 21.35 eV is only 2.4×10^2 . Moreover, the $3d^7 \text{}^4\text{P}$ term is only ≈ 1.7 eV above the ground state of the Fe^+ ion and collisions of ground state Fe^+ ions with electrons are likely to contribute significantly to the creation of these metastables.

In the energy range between the levels excited presumably by Ar^+ -ACT with ground state Fe atoms, reaction (1), and the peak corresponding to the Penning excitation of Fe^+ ions by reactions (2), (3), there are a number of levels with radiative de-excitation rates

between 10^2 and 10^3 (see the TR diagram in Figs. 3, 4). Excitation of these levels can occur by charge transfer between Ar^+ ions and *metastable* (excited) iron atoms, i.e., by the reactions (5), (6) below:



while the reaction (5) involves ground state argon ions ($3\text{p}^5 2\text{P}^{\circ}_{3/2}$, $E = 15.76$ eV) and reaction (6) the $3\text{p}^5 2\text{P}^{\circ}_{1/2}$ metastable argon ions ($E=15.94$ eV). The iron atom has a number of metastable states, the transitions of which to the Fe I ground state ($3\text{d}^6 4\text{s}^2 \text{a}^5\text{D}_4$) are either parity-forbidden or spin-forbidden or both. In the plot in Fig. 4, several groups of states are marked, of which higher de-excitation rates were observed than in their vicinity. The sextet states at ≈ 15.6 eV are excited by Ar^+ -ACT with ground state Fe atoms, reaction (1), as discussed above. The other groups of states marked in Fig. 4 are listed in Table 2, rows 2-3, together with their energies and spin multiplicities ($2S+1$). For these groups of states, charge transfer reactions of the type (5), (6) were found that are likely to be responsible for their excitation: the corresponding energy decrements ΔE are sufficiently small and multiplicities of those states are such that total spin in these reactions is conserved. Such reactions are represented by the corresponding energy decrements and listed in Table 2. Reactions with argon *metastable* ions, Eqn. (6), are specified by the sign *, referring to a remark under the table, and all other suggested reactions are of the type (5), with argon ground state ions. Table 2 shows the terms of Fe I, not individual metastable levels. Each energy decrement ΔE in Table 2 corresponds to an ACT reaction with Fe atom in the state with the lowest energy in the term, which has also the highest quantum number J and thus the highest statistical weight. One more remark to be made is that the combined de-excitation rate of all levels presumably excited by Ar^+ -ACT ($E=15.4$ - 18.6 eV) is $\approx 82\%$ of the total de-excitation rate of all observed Fe II transitions and the combined de-excitation rate corresponding to Ar^+ -ACT with the ground state Fe atoms only (15.4 - 15.9 eV) is $\approx 77\%$. This means that $\approx 4/5$ of all photons in the Fe II spectrum in argon discharge come from Fe ions created by the Ar^+ -ACT reaction.

What remains to be discussed are the Fe II levels between 12.6 and 13.8 eV. Transitions involving these levels exhibit a very similar pattern in argon and neon discharges. The Fe II TR diagram for a glow discharge in neon is in Fig. 5: see the quartet and sextet levels around 13 eV in the upper part of the diagram and compare with those levels in the TR diagram for argon discharge in Fig. 3. Therefore, in the following section, excitation of those levels in both discharge gases is discussed together.

4.2. Fe II levels between 12.6 and 13.8 eV in argon and neon discharges

Because excitation of those levels in both discharge gases is similar, the excitation mechanism will not be a selective one, tied to certain characteristic energy of argon or neon. Zhang et al. reported¹³ that populations of these levels in an argon discharge follow the Boltzmann distribution with a temperature of ≈ 6500 K. This would imply that conditions close to local thermodynamic equilibrium (LTE)²⁵ should exist for those levels. To confirm or dismiss this hypothesis, excitation functions in this energy region were determined also from our data, both for argon and neon discharges (see Figs 6 and 7). The Boltzmann distribution²⁵ can be expressed as

$$\frac{n_2}{n_1} = \frac{g_2}{g_1} e^{\frac{-\Delta E}{kT}} \quad (7)$$

where n_1 , n_2 are populations of two atomic or ionic levels with excitation energies E_1 , E_2 and statistical weights g_1 , g_2 , T is excitation temperature, k is the Boltzmann constant and $\Delta E = E_2 - E_1$. Intensity I_{ik} of a line corresponding to a transition $i \rightarrow k$ is

$$I_{ik} = n_i A_{ik} \frac{hc}{\lambda_{ik}} \quad (8)$$

where A_{ik} is the transition probability, λ_{ik} is the wavelength of that line, h is the Planck constant, c is the speed of light and n_i is the population of the upper level i of that transition. In a Boltzmann plot, the quantity $hc \cdot n_i/g_i = \lambda_{ik} I_{ik}/g_i A_{ik}$ is plotted as a function of energy E_i , on a logarithmic scale. Such a plot may not be necessarily linked to a certain Boltzmann distribution and can be understood in a more general meaning simply as the excitation function plotted with a logarithmic ordinate scale. As such, it is a legitimate tool for studying general population distributions. It should be noted that only if the points in such plot were to follow a straight line with a negative slope, can it be inferred that the plot reflects some kind of thermodynamic equilibrium, with temperature inversely proportional to the slope of that line. Excitation functions derived from our data are in Figs. 6, 7 and do not exhibit such a feature. The dashed line in Fig. 6 is only to show what Zhang et al. reported to be a good linear fit to their data¹³ and is not a linear fit to our data. Zhang et al. worked with different discharge parameters (a 8-mm diameter anode, 800 V, 30 mA) and used fewer lines, spanning over a narrower wavelength range to avoid the need for determining the change with wavelength of the sensitivity of their instrument. Transition probabilities used to calculate the excitation functions in Figs. 6, 7 were taken from the work by Fuhr and Wiese³³. From the plots in Figs. 6, 7 it is apparent

that the level populations do *not* follow a clear trend as function of energy and any 'temperature' based on a certain limited group of lines is meaningless. Probably the most appropriate statement about these excitation functions is that they do not depend much on energy in this region, certainly not in a way that would justify introduction of a 'temperature' in the order of 10^3 - 10^4 K. The points in Fig. 7 are less scattered than in Fig. 6. This is probably because the corresponding lines are much stronger in a neon discharge than in argon (≈ 10 times) and the uncertainty associated with the measured intensities is thus smaller. It is difficult to estimate the uncertainties of individual points in both plots. Some considerations of this kind will be given in the forthcoming paper on a new catalogue of glow discharge spectra, mentioned above in §3.

The Fe^+ ion has a number of metastable states between ≈ 10.7 eV and 12.6 eV, the radiative decay of which is parity-forbidden and which belong e.g. to the following terms: a sextet, $3d^5 4s^2 \text{ } ^6\text{S}$ (10.79 eV), a number of quartets (up to 11.1 eV) and a number of doublets, up to 12.6 eV. These metastable levels are populated by radiative decay of higher excited states (see the lower part of the TR diagrams in Figs. 3, 5) and presumably also by collisions of electrons with Fe^+ ions. A hypothesis may be suggested that collisions with electrons of these metastables contribute significantly to the excitation of the Fe II levels between 12.6 and 13.8 eV investigated here. For LTE to exist for these states, electron density would have to be sufficiently high to prevent the would-be collisional equilibrium with electrons from being perturbed by radiative decay of these states²⁵. That is apparently not the case here, as follows from the excitation functions in Figs. 6, 7.

4.3. Fe II spectrum in an argon-hydrogen discharge

A TR diagram of Fe II in an Ar(H) discharge is in Fig. 8. Compared with the TR diagram for a discharge in pure argon (Fig. 3), the most apparent feature is that the peak at ≈ 15.6 eV and vicinity, corresponding to the Ar^+ -ACT reaction, is greatly suppressed, whilst the other groups of states are either not suppressed or suppressed to a much lesser extent. Many weak lines from the discharge in argon were not observed in the Ar(H) discharge, which is the reason why many Fe II levels with low de-excitation rates, displayed in Fig. 3, are missing in Fig. 8. A clearer picture is given in Fig. 9 in which ratios of de-excitation rates in Ar- and Ar(H) discharge are plotted with a linear ordinate scale as a function of energy of the Fe II levels. As mentioned above, transition rates are corrected for a different sputtering rate of iron in both discharges, by a factor $q_{\text{Ar(H)}}(\text{Fe})/q_{\text{Ar}}(\text{Fe}) = 0.77^{18,34}$. Hence, in an approximation of negligible collisional de-excitation, the plot in Fig. 9 can be interpreted as relative probability of a level to be excited in Ar(H) discharge, compared to argon discharge. The plot in Fig. 9 is in

good agreement with the results described by Steers et al.¹⁸ and gives more information than Ref.¹⁸ for levels above 18 eV. The Ar(H)/Ar factors of ≈ 0.15 - 0.25 were observed for all levels that are close to 15.6-15.8 eV, including the doublet levels. Hydrogen greatly reduces the population of Ar^+ ions, creating ArH^+ ions instead³⁵ and reducing thereby the rate of the Ar^+ -ACT reactions in the discharge³⁶. This is the case here. It is remarkable that the Fe II *doublet* levels that are close to the resonance energy for Ar^+ -ACT also behave in the same manner as the quartet and sextet levels for which the Ar^+ -ACT reaction preserves spin. The levels between 12.6 and 13.8 eV, described earlier under §4.2, split into two groups, of which the sextet levels, with lower energies, are suppressed and the quartet levels are not. They exhibit a peak in the vicinity of 13.6 eV, the ionization energy of hydrogen. This behaviour was also described by Steers et al.¹⁸ and attributed to charge transfer reaction between iron atoms and H^+ ions.

The Fe II levels around 18 eV, excited presumably by Ar^+ -ACT with iron metastables (Table 2) are also slightly suppressed in Ar(H) discharge but less than those around 15.6-15.8 eV mentioned above. Finally, most of the levels around 19.5 eV excited by Penning excitation of Fe^+ ions by argon metastables, Eqns (2), (3), are virtually unaffected by the addition of hydrogen. Lines associated with transitions from those levels are weak (see Fig. 3), which causes increased uncertainties of the measured intensities and the scatter of the points around 19.5 eV in Fig. 9.

4.4. Fe II spectrum in a neon discharge

A TR diagram of Fe II in neon discharge is in Fig. 5 and an initial discussion of its implications is given in this section. As in the case of the Ar(H) discharge, transition rates were corrected for a different sputtering rate of iron in argon and neon discharges, with a factor $q_{\text{Ne}}(\text{Fe})/q_{\text{Ar}}(\text{Fe}) = 0.45$, and the TR diagrams for argon and neon discharge in this paper can thus be compared on a quantitative basis. One result that can be derived from such comparison is e.g. that the combined de-excitation rate corresponding to all observed transitions in the spectrum (i.e. the number of emitted photons per certain number of sputtered iron atoms) is 3.9×10^5 units in argon discharge and 1.8×10^6 in neon, i.e., 4.6 times bigger.

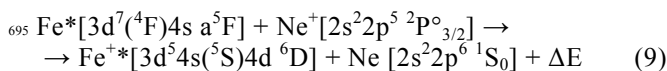
Excitation of the low-energy Fe II states at ≈ 12.6 - 13.8 eV was discussed in §4.3. The ionization energy of neon is 21.56 eV and the difference between the TR diagrams in argon (Fig. 3) and neon (Fig. 5) suggests that the Ne^+ -ACT reaction with iron plays a very significant role in populating Fe II levels above ca 20.6 eV. A large number of levels with de-excitation rates $>10^3$ spans from ≈ 20.6 to 21.6 eV, which is a much wider interval than the width of the peak in the TR diagram in Fig. 3, corresponding to the Ar^+ -ACT reaction. We observed a

1
2 similar phenomenon for manganese¹⁴. An expanded
3 section of the Fe II TR diagram in neon discharge,
4 spanning the energy range from 19 to 23 eV, is shown
5 in Fig. 10, together with a diagram depicting energies of
6 all existing Fe II levels in that interval, sorted by their
7 spin multiplicity. It is remarkable that the strongly
8 excited levels also include some *octet* states at 21.1–
9 21.5 eV, close to the resonance energy for Ne⁺-ACT,
10 but not compatible with the requirement of spin
11 conservation in the Ne⁺-ACT reaction with ground state
12 Fe atoms. This particularly concerns the 3d⁵(⁶S)4p² ⁸P
13 term at 21.1-21.2 eV. A closer look shows that *all*
14 existing Fe II *octet* states within a ≈1eV-wide energy
15 interval below the ionization energy of neon are excited,
16 whilst the levels that are closer to the neon ionization
17 energy, belonging to the term 3d⁵4s(⁷S)4d ⁸D (21.47
18 eV), are much less excited than those at 21.1-21.2 eV
19 (3d⁵4p² ⁸P). Also, there are a number of *doublet* levels,
20 relatively strongly excited, in that energy range. They
21 also do not comply with the Wigner spin rule for direct
22 Ne⁺-ACT reaction with ground state Fe atoms. Many of
23 them decay by inter-combination transitions to sextet
24 levels at 18.2-18.4 eV, with the wavelengths of the
25 corresponding lines around 500 nm. A notable feature in
26 the plot in Fig. 10 is a peak at ≈20.7 eV of the Fe II
27 doublet levels. To determine accurately the relations
28 between deexcitation rates of levels with different
29 multiplicities in the vicinity of the resonance energy for
30 the Ne⁺-ACT reaction, a very good radiometric
31 calibration is needed: the strongly excited *octet* levels at
32 21.1-21.2 eV of the term 3d⁵(⁶S)4p² ⁸P decay by
33 transitions in the vacuum ultraviolet (VUV) region, the
34 sextet levels by transitions in a wide range from VUV to
35 ≈ 360 nm, the quartets largely by transitions around
36 230-240 nm and the doublets mostly by transitions in
37 the visible region around 500 nm. Estimated uncertainty
38 of the radiometric calibration used in this study may be
39 up to ≈30% relative in some narrow wavelength regions.
40 Despite that, the plot in Fig. 10 gives a reasonably good
41 basic view of the situation.

42 For comparison with the Fe-Ar⁺ ACT reaction, an
43 expanded section of the Fe II TR diagram in argon
44 discharge is shown in Fig. 11, in the range of 12-16 eV,
45 i.e., spanning over the energy interval width of 4 eV as
46 in the plot in Fig. 10. The peak corresponding to Ar⁺-
47 ACT (Fig. 11) is much narrower than the energy
48 interval supposedly related to Ne⁺-ACT (Fig. 10). This
49 may be largely due to different distributions of Fe II
50 states with suitable multiplicities below the resonance
51 energies for both charge transfer reactions (see Figs. 10,
52 11). But, for example, the 3d⁵4s² d⁴P term (15.02-15.04
53 eV) is clearly out of the energy region where the Ar⁺-
54 ACT reaction operates, as no lines originating from its
55 levels were observed in the spectrum (these would be
56 lines of the 3d⁵4s² d⁴P - 3d⁶(⁵D)4p z⁴F^o multiplet, λ ≈
57 771-800 nm).

58 The sextet states at 22.32 eV with de-excitation rates of
59 6x10² to 1.7x10³ units in the TR diagram in Fig. 10 can
60

be excited by a Ne⁺-ACT reaction with metastable iron
atoms, in analogy to the reactions (5), (6), occurring in
argon discharge. Full classification of the reacting
species is as follows:



The energy decrement ΔE in reaction (9) is 0.10 eV. Fe
II levels below ca 18.5 eV are subject to massive
cascade excitation from higher levels. For example, the
quartet levels at ≈15.5-16.2 eV have comparable rates of
cascade excitation and de-excitation, suggesting that
collisional excitation probably plays only a small role
for them. Therefore, any considerations concerning
collisional excitation in this region must be made with
705 caution and based on *net de-excitation rates*, i.e., with
the cascade excitation rates of these levels subtracted.

This section is to be considered only as an introduction
to excitation processes of iron ions in a neon discharge.
Further work would be required to obtain a more
710 complete picture.

5. Summary and conclusions

Besides the plots of intensity ratios of emission lines as
a function of energy, there are two major tools for
715 describing excitation processes, based on information
that can be derived from emission spectra: the TR
diagrams and the Boltzmann plots. TR diagrams were
defined in §2 and Boltzmann plots were mentioned in
§4.3. It is worthwhile summarizing here their
similarities and differences, which is done in Table 3.
720 Boltzmann plots are more useful in describing higher
power atmospheric discharges, such as ICP, than a glow
discharge, because, at a higher pressure, collisional
processes dominate the excitation/de-excitation paths
and conditions close to local thermodynamic
725 equilibrium are more likely to occur. The present study
uses largely TR diagrams.

The process that dominates excitation of the Fe II
spectrum both in argon and neon glow discharges is the
asymmetric charge transfer reaction between ions of the
730 discharge gas and neutral iron atoms. Besides ground
state Fe atoms, charge transfer reactions with argon and
neon ions were confirmed also for a number of Fe I
metastable states. In the case of Ar⁺-ACT, the Fe I
metastables up to the energy of ≈2.9 eV are involved.
735 Sextet levels at ≈15.60 eV are more strongly excited by
Ar⁺-Fe charge transfer, than quartet levels with almost
the same energy. There are differences between Ar⁺-Fe
and Ne⁺-Fe charge transfer reactions, the latter leading
740 to a much wider range of strongly excited Fe II levels
(≈20.6-21.6 eV) than the Ar⁺-Fe reaction (≈15.5-15.9
eV). This is partly due to the distribution of energy
levels of appropriate energy and multiplicity. Also, in
the neon discharge, a number of strongly excited
745 doublet and octet Fe II states was observed with

energies close to the neon ionization energy. If they are excited by Ne⁺-ACT, it would mean that the Wigner spin rule, according to which the combined spin of reacting particles is conserved, is violated in the Ne⁺-ACT reaction. In argon discharge, this might concern some doublet Fe II levels close to the argon ionization energy. But their radiative de-excitation rates are by two orders of magnitude lower than those of the most strongly excited levels. The Ar⁺-ACT reaction is strongly suppressed by small amounts of hydrogen. This has consequences for analytical methodology, namely, that the strong Fe II lines of the y⁶P^o-a⁶D multiplet, λ=161-163 nm, are very sensitive to the presence of hydrogen, either as an impurity in the argon plasma (from moisture) or coming from the analyzed sample.

Besides charge transfer, also other selective reactions were identified, occurring only at narrow energy intervals. They include Penning excitation of ground state- and metastable Fe⁺ ions by argon metastables. All these reactions produce characteristic peaks at the corresponding energies in the TR diagrams.

The lowest levels contributing to Fe II emission spectrum, at energies 12.6-13.8 eV, are probably mainly excited by electronic collisions, besides radiative decay of higher excited states. Contrary to the earlier work by Zhang et. al.¹³, no evidence was found for any kind of local thermodynamic equilibrium in this energy region. Hence, any 'temperatures', as derived from Fe II glow discharge emission spectra, are meaningless. Prospects to find conditions close to LTE may exist for the lowest (metastable) Fe II levels, the populations of which could be possibly determined by absorption measurements.

The processes mentioned above can satisfactorily explain excitation of the Fe II spectrum in argon discharge. The Fe II spectrum in a neon glow discharge is much more complex, due to cascade processes (excitation by radiative decay of higher Fe II levels). A detailed study of prospective selective excitation reactions for Fe II levels below ca 18.5 eV in neon discharges would be therefore much more difficult than in an argon discharge.

To summarise, the excitation of Fe⁺ ions in argon-, neon- and argon-hydrogen glow discharges has been described, based on the formalism of transition rate diagrams. The data presented here can be used as basis for collisional-radiative models of iron in glow discharge plasmas and to compare the predictions of such models with experimental data.

References

- 1 K.R. Marcus and J.A.C. Broekaert, *Glow Discharge Plasmas in Analytical Spectroscopy*, John Wiley & Sons, Chichester, 2003
- 2 R.E. Steiner, C.M. Barshick, A. Bogaerts, *Glow Discharge Optical Spectroscopy and Mass Spectro-*

- metry, in: R.A. Meyers (Ed.), *Encyclopedia of Analytical Chemistry*, J.Wiley & Sons Ltd, 2009
- 3 P.W.J.M. Boumans, *Theory of Spectrochemical Excitation*, Hilger & Watts, London 1966
- 4 Amoroso S., Bruzzese R., Spinelli N., Velotta R. Characterization of laser ablation plasmas, *Journal of Physics B: At. Mol. Opt. Phys.* 1999, **32**, R131
- 5 H. Haraguchi, T. Hasegawa, M. Abdullah, Inductively coupled plasmas in analytical atomic spectrometry: excitation mechanisms and analytical feasibilities, *Pure & Appl. Chem.*, 1988, **60**, 685
- 6 Z. Weiss, Glow discharge excitation and matrix effects in the Zn-Al-Cu system in argon and neon, *Spectrochim. Acta Part B*, 2007, **62**, 787.
- 7 E.B.M. Steers and J. Fielding, Charge-transfer excitation processes in the Grimm lamp, *J. Anal. At. Spectrom.*, 1987, **2**, 239
- 8 E.B.M. Steers and A. Thorne, Application of high resolution Fourier transform spectrometry to the study of glow discharge sources. 1. Excitation of iron and chromium spectra in a microwave-booster glow discharge source, *J. Anal. At. Spectrom.*, 1993, **8**, 309
- 9 S. Mushtaq, E.B.M. Steers, J.C. Pickering and K. Putyera, Selective and non-selective excitation/ionization processes in analytical glow discharges: excitation of the ionic spectra in argon/helium mixed plasmas, *J. Anal. At. Spectrom.*, 2014, **29**, 681
- 10 G.C.-Y. Chan, G.M. Hieftje, Using matrix effects as a probe for the study of the charge-transfer mechanism in inductively coupled plasma-atomic emission spectrometry, *Spectrochim. Acta, Part B*, 2004, **59**, 163
- 11 K. Wagatsuma, R. Oka and S. Urushibata, Excitation processes in introduction of bias current to a radio-frequency glow discharge plasma evaluated from Boltzmann plots of iron atomic and ionic spectral lines, *Anal. Sci.*, 2012, **28**, 759
- 12 L. Zhang, S. Kashiwakura and K. Wagatsuma, Boltzmann statistical consideration on the excitation mechanism of iron atomic lines emitted from glow discharge plasmas, *Spectrochim. Acta, Part B*, 2011, **66**, 785
- 13 L. Zhang, S. Kashiwakura and K. Wagatsuma, Deviation from Boltzmann distribution in excited energy levels of singly-ionized iron in an argon glow discharge plasma for atomic emission spectrometry, *Spectrochim. Acta, Part B*, 2012, **67**, 24
- 14 Z. Weiss, E.B.M. Steers, J.C. Pickering and S. Mushtaq, Transition rate diagrams — A new approach to the study of selective excitation processes: The spectrum of manganese in a Grimm-type glow discharge, *Spectrochim. Acta, Part B*, 2014, **92**, 70
- 15 S. Johansson, U. Litzén, Possibilities of obtaining laser action from singly ionised iron group elements through charge transfer in hollow cathode lasers *J. Phys. B*, 1980, **13**, L253
- 16 E.B.M. Steers and J. Leis, Excitation of the spectra of neutral and singly ionized atoms in the Grimm-type discharge lamp, with and without supplementary microwave excitation, *Spectrochim. Acta, Part B*, 1991, **46**, 527
- 17 K. Wagatsuma, K. Hirokawa, Classification of singly ionized iron emission lines in the 160-250 nm wavelength region from Grimm-type glow discharge plasma, *Spectrochim. Acta, Part B*, 1996, **51**, 349
- 18 E.B.M. Steers, P. Šmíd, Z. Weiss, Asymmetric charge transfer with hydrogen ions — an important factor in the

- 1
2 “hydrogen effect” in glow discharge optical emission
3 spectroscopy, *Spectrochim. Acta Part B*, 2006, **61**, 414 905
4
5 19 P. Šmíd, E.B.M. Steers, Z. Weiss, J. Pickering and V.
6 Hoffmann, The effect of hydrogen and nitrogen on
7 emission spectra of iron and titanium atomic lines in
8 analytical glow discharges, *J. Anal. At. Spectrom.*,
9 2008, **23**, 1223 910
10
11 20 S. Johansson, *Physica Scripta*, 2009, T134, 014013
12 doi:10.1088/0031-8949/2009/T134/014013 875
13
14 21 G. Nave and S. Johansson, The spectrum of Fe II,
15 *Astrophys. J. Suppl. Ser.*, 2013, **204**:1
16
17 22 I. Korolov, G. Bánó, Z. Donkó, A. Derzsi, P.
18 Hartmann, Experimental study of the asymmetric
19 charge transfer reaction between Ar⁺ ions and Fe
20 atoms, *J. Chem. Phys.*, 2011, **134**, 064308 880
21
22 23 Z. Weiss, Emission yields and the standard model in
23 glow discharge optical emission spectroscopy: links to
24 the underlying physics and analytical interpretation of
25 the experimental data, *Spectrochim. Acta Part B*, 2006,
26 **61**, 121 885
27
28 24 J. C. Pickering, High resolution Fourier transform
29 spectroscopy with the Imperial College (IC) UV-FT
30 spectrometer, and its applications to astrophysics and
31 atmospheric physics: a review, *Vibrational*
32 *Spectroscopy*, 2002, **29**, 27 890
33
34 25 A. Thorne, U. Litzén and S. Johansson, *Spectrophysics:*
35 *Principles and Applications*, Springer, 1999 930
36
37 26 J.C. Pickering, S. Johansson, P.L. Smith, The FERRUM
38 project: Branching ratios and atomic transition
39 probabilities of Fe II transitions from the 3d⁶(a³F)4p
40 subconfiguration in the visible to VUV spectral region,
41 *Astronomy and Astrophysics*, 2001, **377**, 361 895
42
43 27 S. D. Bergeson, K. L. Mullman, M.E. Wickliffe, J. E.
44 Lawler, U. Litzén, S. Johansson, Branching fractions
45 and oscillator strengths for Fe II transitions from the
46 3d⁶(⁵D)4p subconfiguration, *The Astrophysical Journal*,
47 1996, **464**, 1044 900
48
49
50
51
52
53
54
55
56
57
58
59
60
- 28 A. Kramida, Yu. Ralchenko, J. Reader and NIST ASD
Team (2013). NIST Atomic Spectra Database (ver.
5.1), [Online]: <http://physics.nist.gov/asd> [2014, May
10]. National Institute of Standards and Technology,
Gaithersburg, MD
29 T. R. O'Brian, M. E. Wickliffe, J. E. Lawler, W.
Whaling, J.W. Brault, Lifetimes, transition probabilities
and level energies in Fe I, *J. Opt. Soc. Am. B*, 1991, **8**,
1185
30 Z. Weiss, E.B.M. Steers, P.Šmíd and V. Hoffmann,
Towards a catalogue of glow discharge emission
spectra, *J. Anal. At. Spectrom.*, 2009, **24**, 27
31 N. Jakubowski, E. Steers, A. Tempez, Glow and Glory,
J. Anal. At. Spectrom., 2007, **22**, 715
32 K. Marshall, P. M. Willis, Centered Sphere Spectro-
meter, US Patent 6023330
33 J.R. Fuhr, W.L. Wiese, A critical compilation of atomic
transition probabilities for atomic and singly ionized
iron, *J. Phys. Chem. Ref. Data*, 2006, **35**, 1669
34 Z. Weiss, E.B.M. Steers, P.Šmíd, Excitation of zinc in a
Grimm-type glow discharge: effects of hydrogen and
other excitation-related matrix effects, *J. Anal. At.*
Spectrom., 2005, **20**, 839
35 P.H. Ratcliff, W.W. Harrison, The effect of water
vapor in glow discharge mass spectrometry,
Spectrochim. Acta, Part B, 1994, **49**, 1747-1757
36 V.-D. Hodoroaba, V. Hoffmann, E.B.M. Steers, K.
Wetzig, Emission spectra of copper and argon in an
argon glow discharge containing small quantities of
hydrogen, *J. Anal. At. Spectrom.* 2000, **15**, 951

Table 1Calculation of radiative excitation / de-excitation rates of the Fe II level $3d^6(^5D)4p z^6P^{\circ}_{3/2}$ in a glow discharge in neon

λ_{ij} / nm	I_{ij} / arb.units	the level from/into *)				transition rate / arb.units	
		E / eV *)	config.	term	J	the line	total
transitions populating the $3d^6(^5D)4p z^6P^{\circ}_{3/2}$ level at 13.3108 eV							
286.412	0.087	17.6384	$3d^6(^5D)5s$	e^6D	5/2	103	8 101
284.778	0.68	17.6632	"	"	3/2	783	
283.822	0.46	17.6779	"	"	1/2	511	
247.640	0.44	18.3159	$3d^6(^5D)4d$	6D	3/2	133	
246.774	1.77	18.3335	"	"	1/2	572	
245.590	6.5	18.3577	"	6P	5/2	2 239	
245.003	5.6	18.3698	"	"	3/2	1756	
238.737	7.7	18.5025	"	6S	5/2	1 947	
158.701	0.094	21.1232	$3d^54s(^7S)4d$	6D	3/2	25	
158.645	0.26	21.1260	"	"	5/2	68	
transitions depopulating the $3d^6(^5D)4p z^6P^{\circ}_{3/2}$ level at 13.3108 eV							
232.740	13	7.9853	$3d^6(^5D)4s$	a^6D	5/2	3196	14 880
233.801	29	8.0094	"	"	3/2	7017	
234.429	19	8.0236	"	"	1/2	4 521	
492.392	0.093	10.7935	$3d^54s^2$	a^6S	5/2	146	

*) the upper level of transitions populating the level $3d^6(^5D)4p z^6P^{\circ}_{3/2}$ and the lower level of transitions depopulating the level $3d^6(^5D)4p z^6P^{\circ}_{3/2}$

Table 2

Possible excitation of some Fe II states by ACT between Ar⁺ ions and Fe metastable atoms (reactions (5), (6)): energy decrements ΔE in eV

			excited Fe II levels observed in emission spectra					
			E / eV	16.47- -16.51	16.91- -16.96	17.73- -17.81	18.19	18.36
2S+1			4	2, 4	4, 6	6	6	4
Fe I metastables								
		E / eV						
3d ⁷ (⁴ F)4s	a ⁵ F	0.85-1.00	0.12					
"	a ³ F	1.49-1.61		(0.29)				
3d ⁷ (⁴ P)4s	a ⁵ P	2.17-2.22			0.16			
3d ⁶ (⁵ D)4s4p(³ P ^o)	z ⁷ D ^o	2.40-2.48				- 0.03, 0.15*		
3d ⁷ (² G)4s	a ³ G	2.69-2.73						0.05*
3d ⁶ (⁵ D)4s4p(³ P ^o)	z ⁷ F ^o	2.81-2.89					0.21	
3d ⁷ (⁴ P)4s	b ³ P	2.83-2.86						0.01, 0.19*

* this energy decrement corresponds to a reaction with argon *metastable* ions (15.94 eV)

Table 3

TR diagrams and Boltzmann plots: an overview

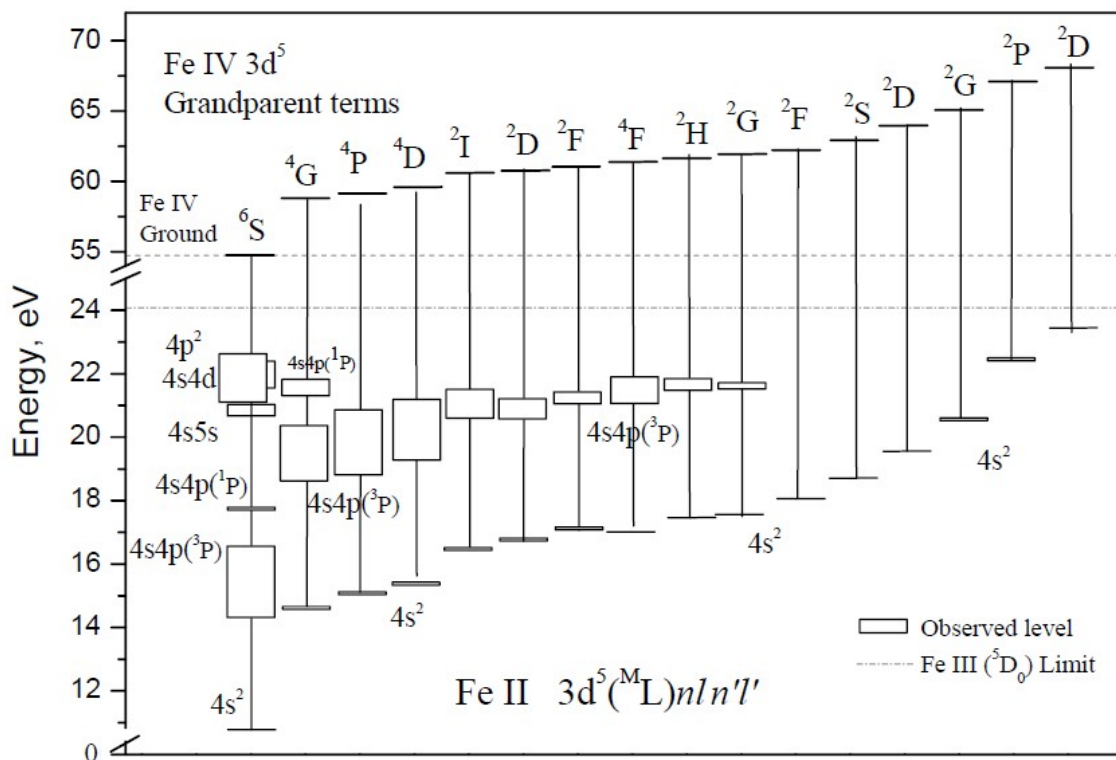
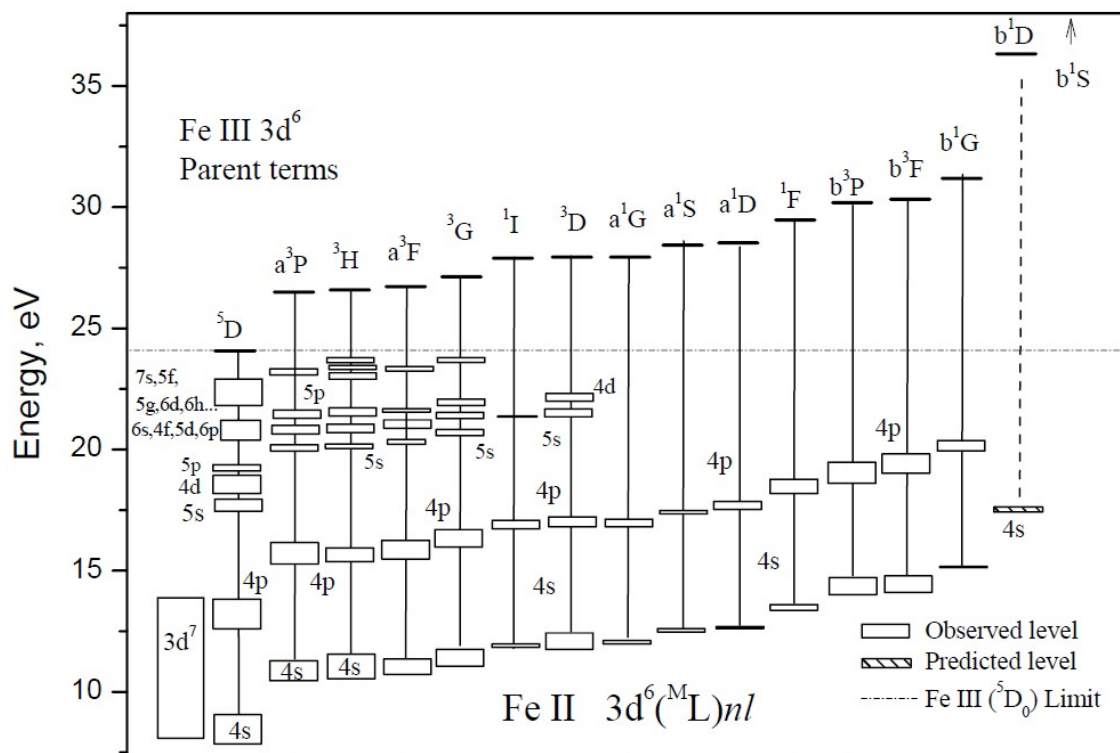
feature	TR diagrams	Boltzmann plots (excitation functions)
the quantity on abscissa	E_i	E_i
the quantity on ordinate	$\sum_i \lambda_{ik} I_{ik}$, $\sum_k \lambda_{ik} I_{ik}$	$\lambda_{ik} I_{ik} / (g_i A_{ik})$
ordinate scale	linear or logarithmic	logarithmic
the points represent	levels (or terms)	observed lines
type of information displayed	relative transition rates	relative populations
brings information about	levels (terms)	upper levels of observed lines
radiometric intensity calibration	needed	needed
extra information required	none	transition probabilities statistical weights of the levels
suitable for investigating	selective collisional excitation cascade processes radiative population rates	existence of LTE excit. temperature if LTE exists
most useful if	RD \gg CD *)	RD \ll CD *)

*) RD = the rate of radiative decay, CD = the rate of collisional de-excitation

Fig. 1

Energy level structure of singly ionized iron.

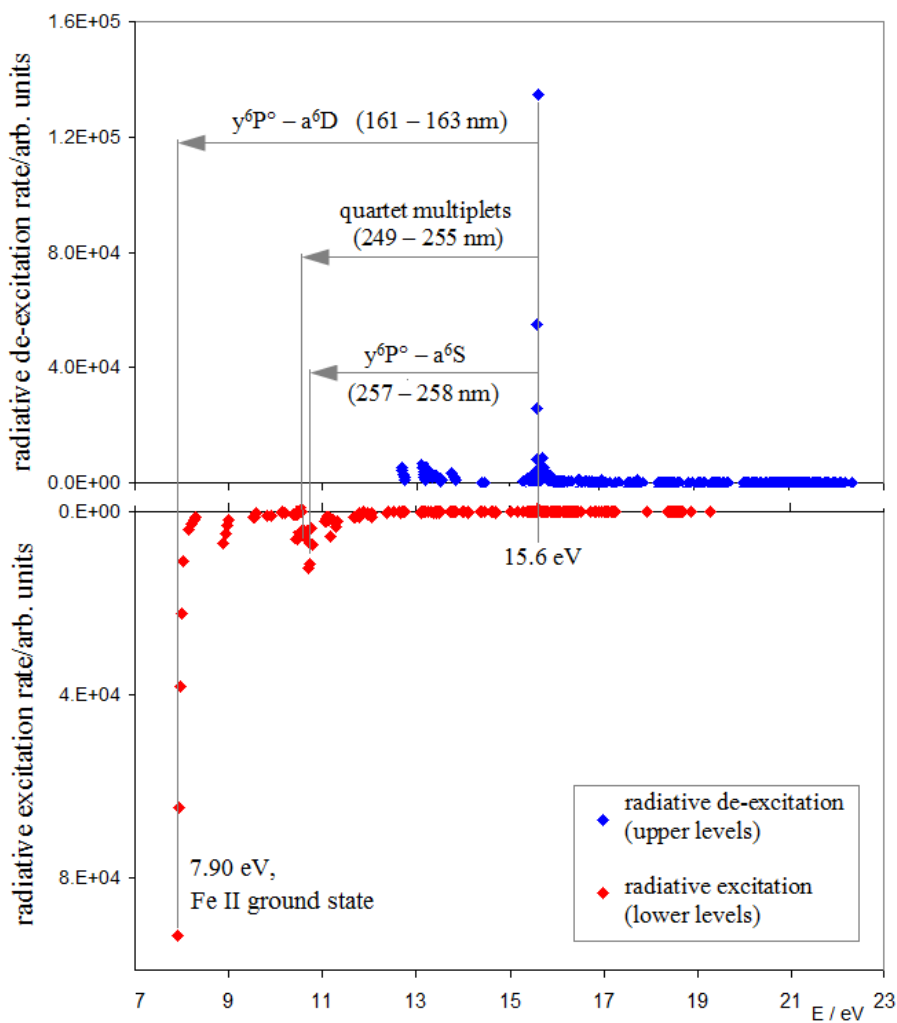
Top: the 'normal' system (singly excited), bottom: the doubly excited system



1
2
3
4
5
6
7
8
9
10
11
12
13
14
15
16
17
18
19
20
21
22
23
24
25
26
27
28
29
30
31
32
33
34
35
36
37
38
39
40
41
42
43
44
45
46
47
48
49
50
51
52
53
54
55
56
57
58
59
60

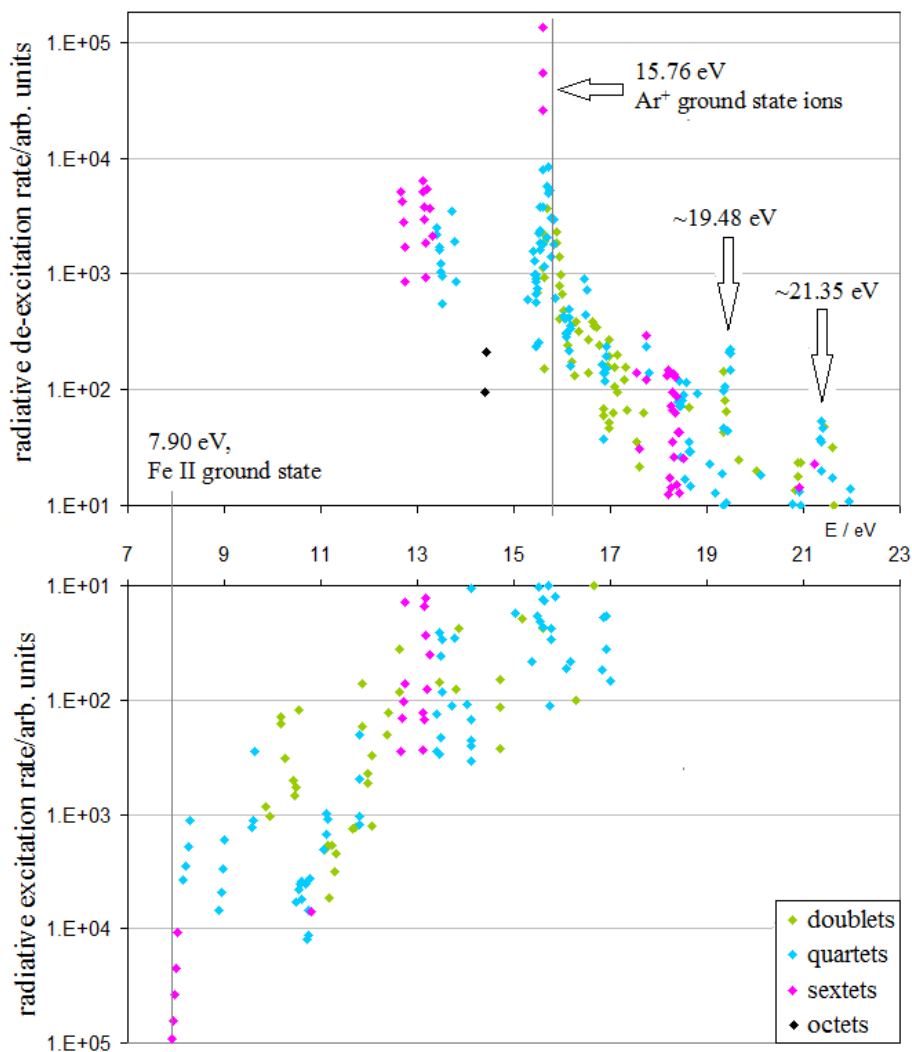
955

Fig. 2
 TR diagram of Fe II in an argon discharge



960

Fig. 3
TR diagram of Fe II in an argon discharge, logarithmic ordinate scale



965

Fig. 4
 Radiative de-excitation rates in argon discharge of Fe II levels with energies between 15 eV and 19 eV
 (note a logarithmic ordinate scale)

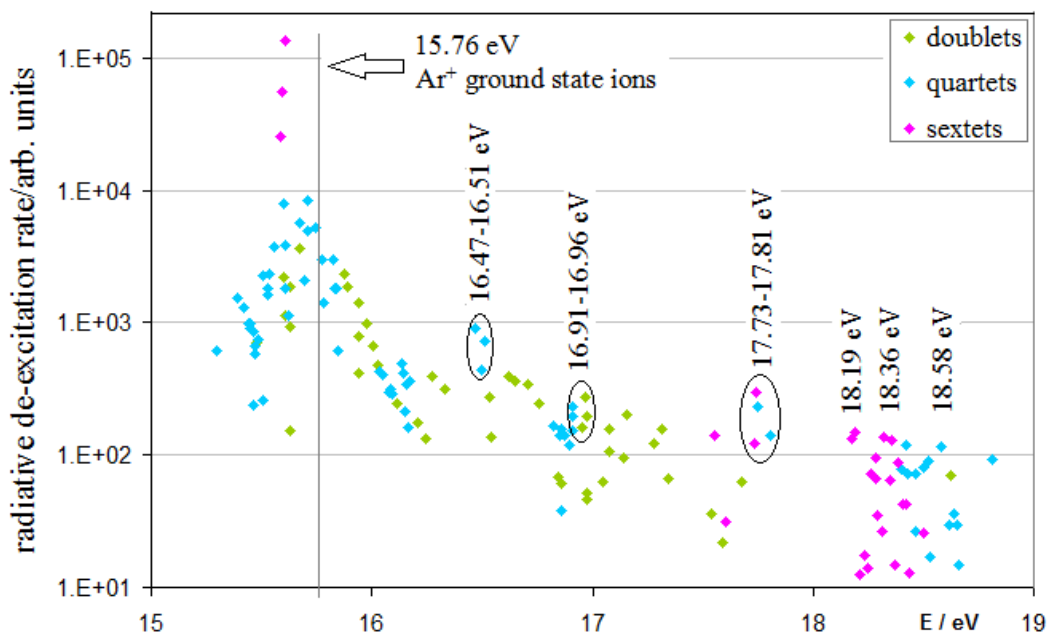
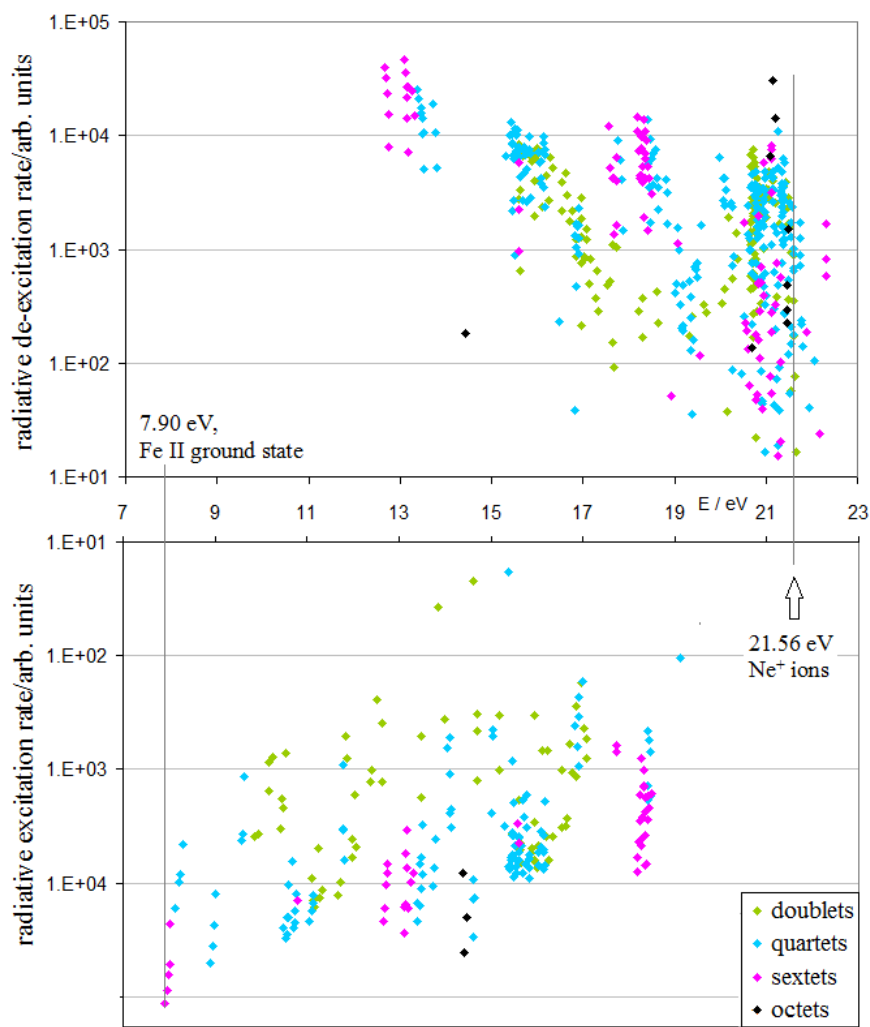


Fig. 5
TR diagram of Fe II in neon discharge



980

Fig. 6

Excitation function for Fe II lines with excitation energies of 12.6 – 13.8 eV in an argon discharge. The dashed line is *not* a linear fit to this data but its gradient corresponds to the “temperature” quoted in Ref.¹³

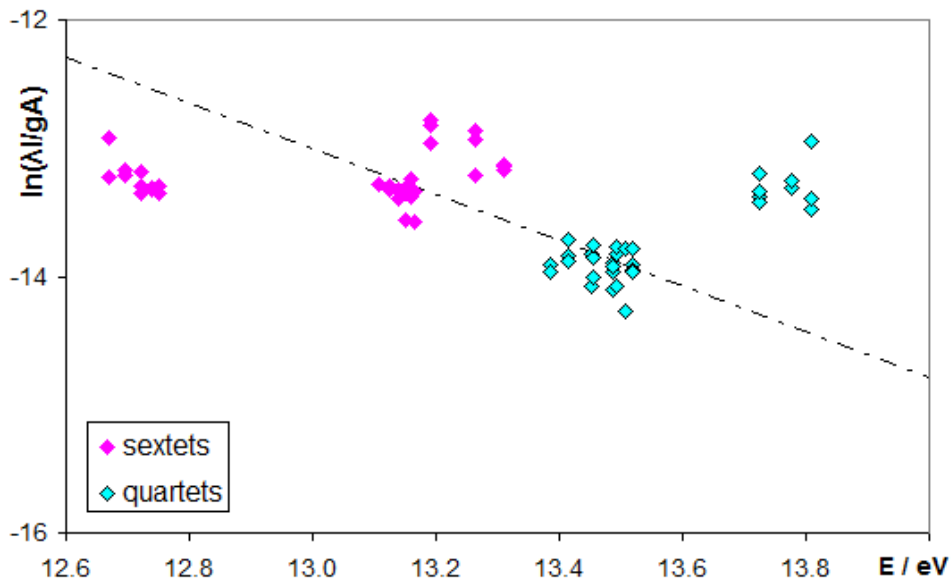


Fig. 7

Excitation function for Fe II lines with excitation energies of 12.6 – 13.8 eV in a neon discharge.

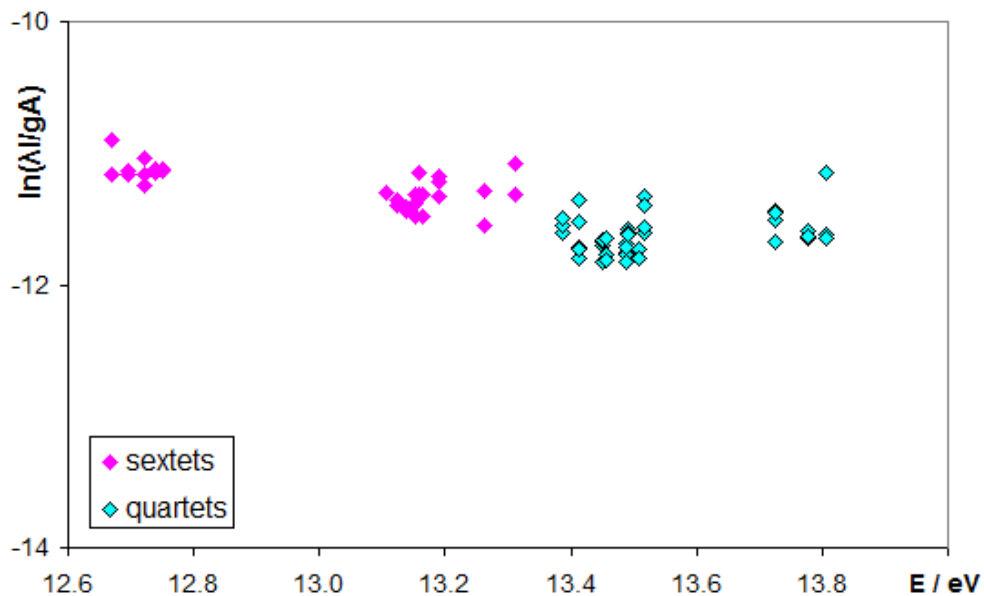


Fig. 8
TR diagram of Fe II in an argon-hydrogen discharge

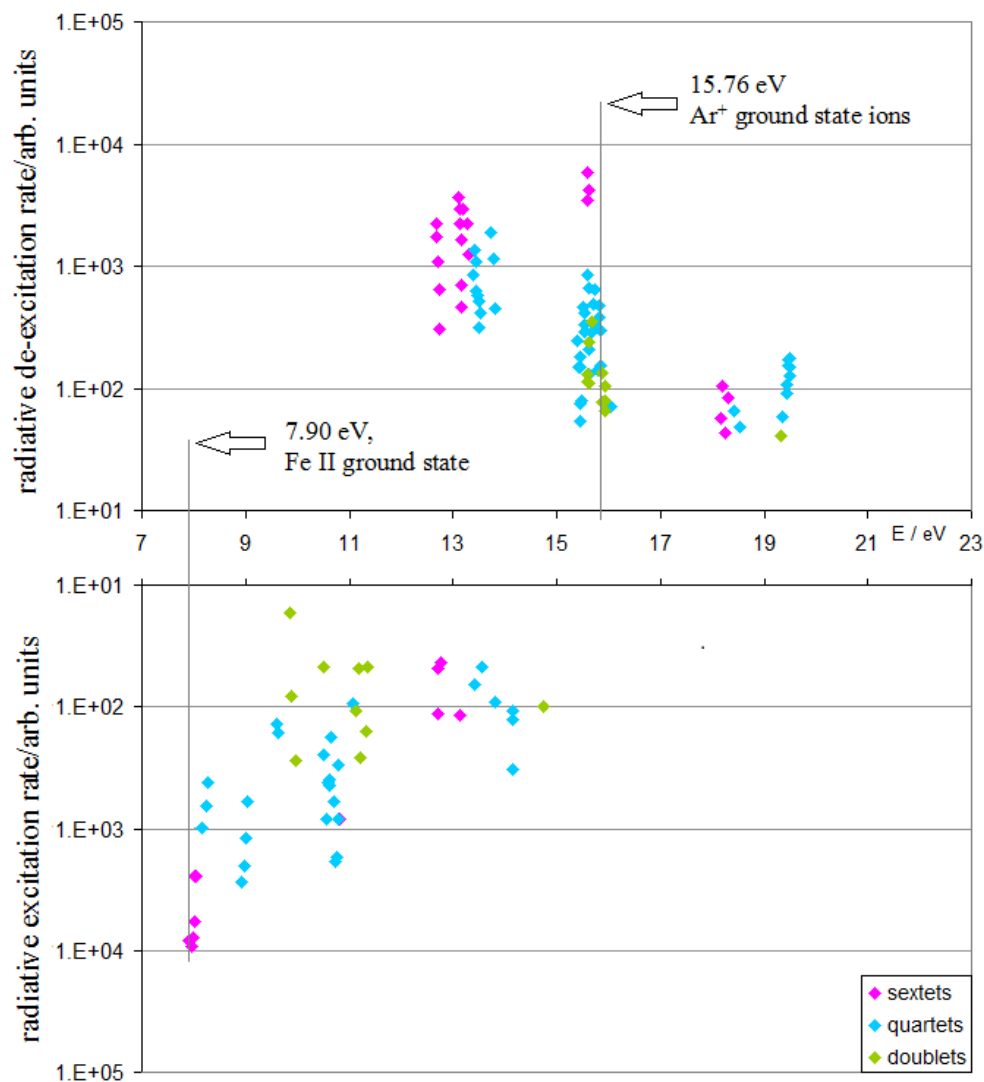


Fig. 9
 TR(Ar+H) / TR(Ar) enhancement factors for Fe II levels

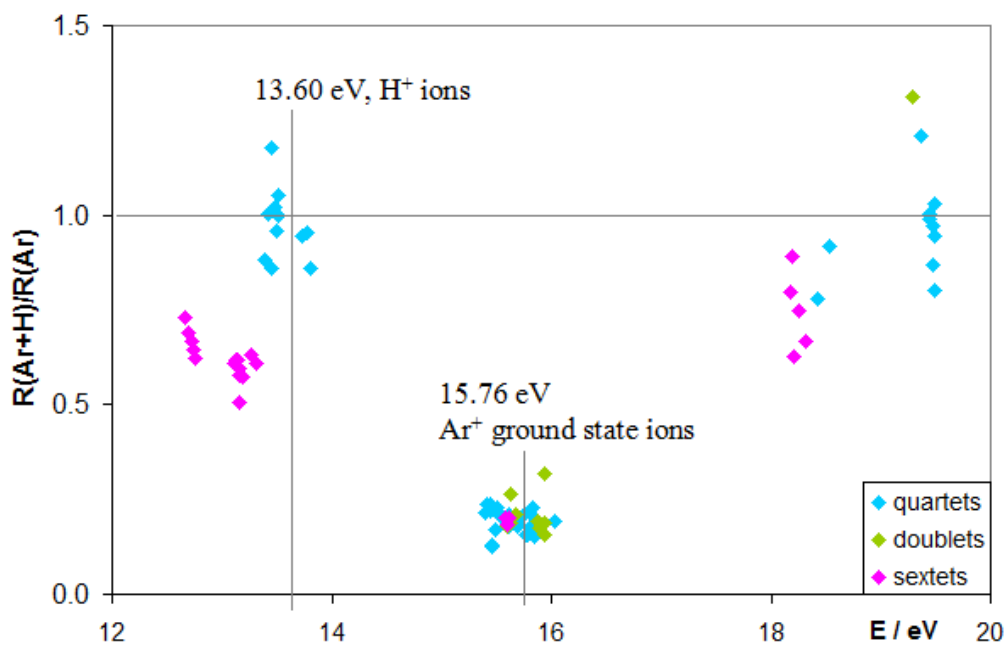


Fig. 10

TR diagram of Fe II in a neon discharge, excitation energies 19-23 eV

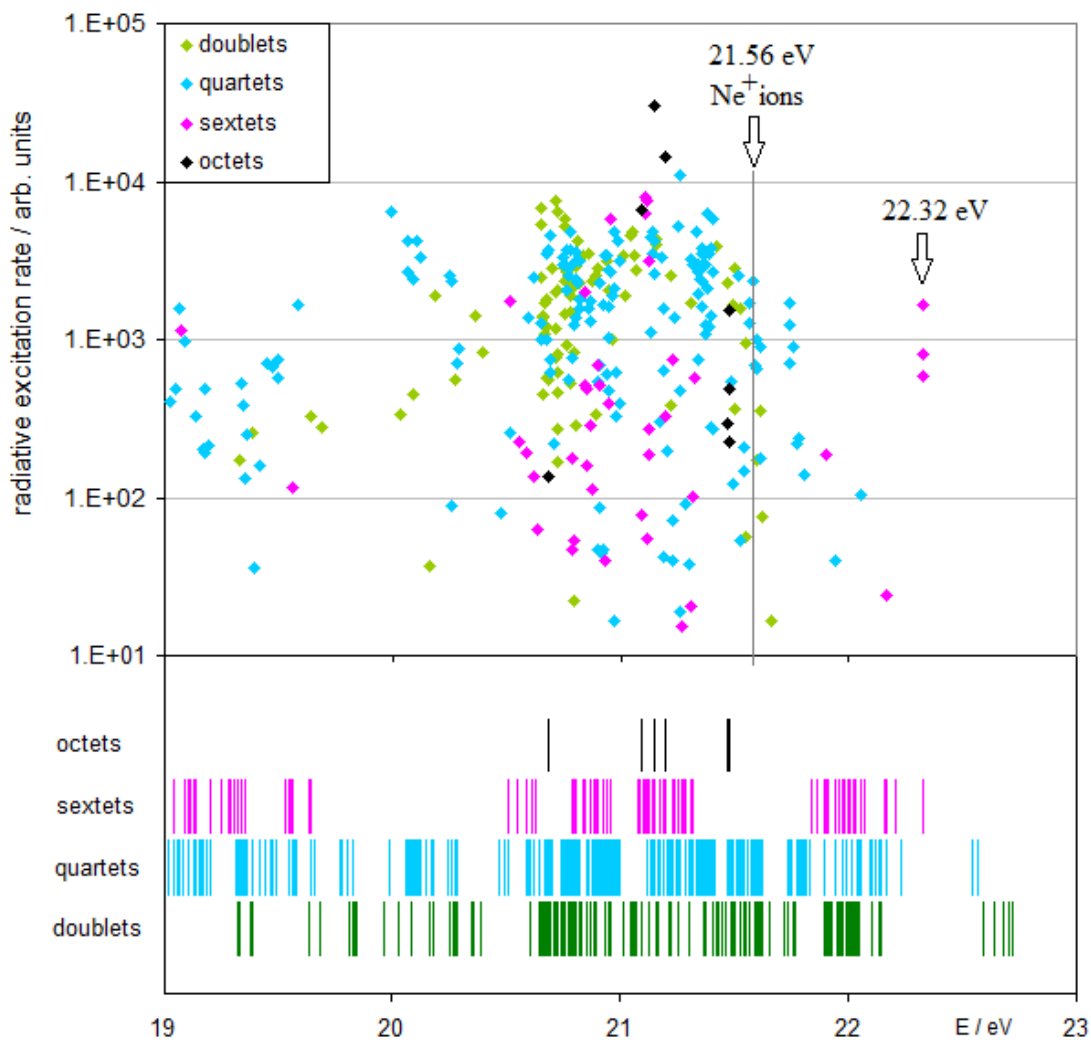
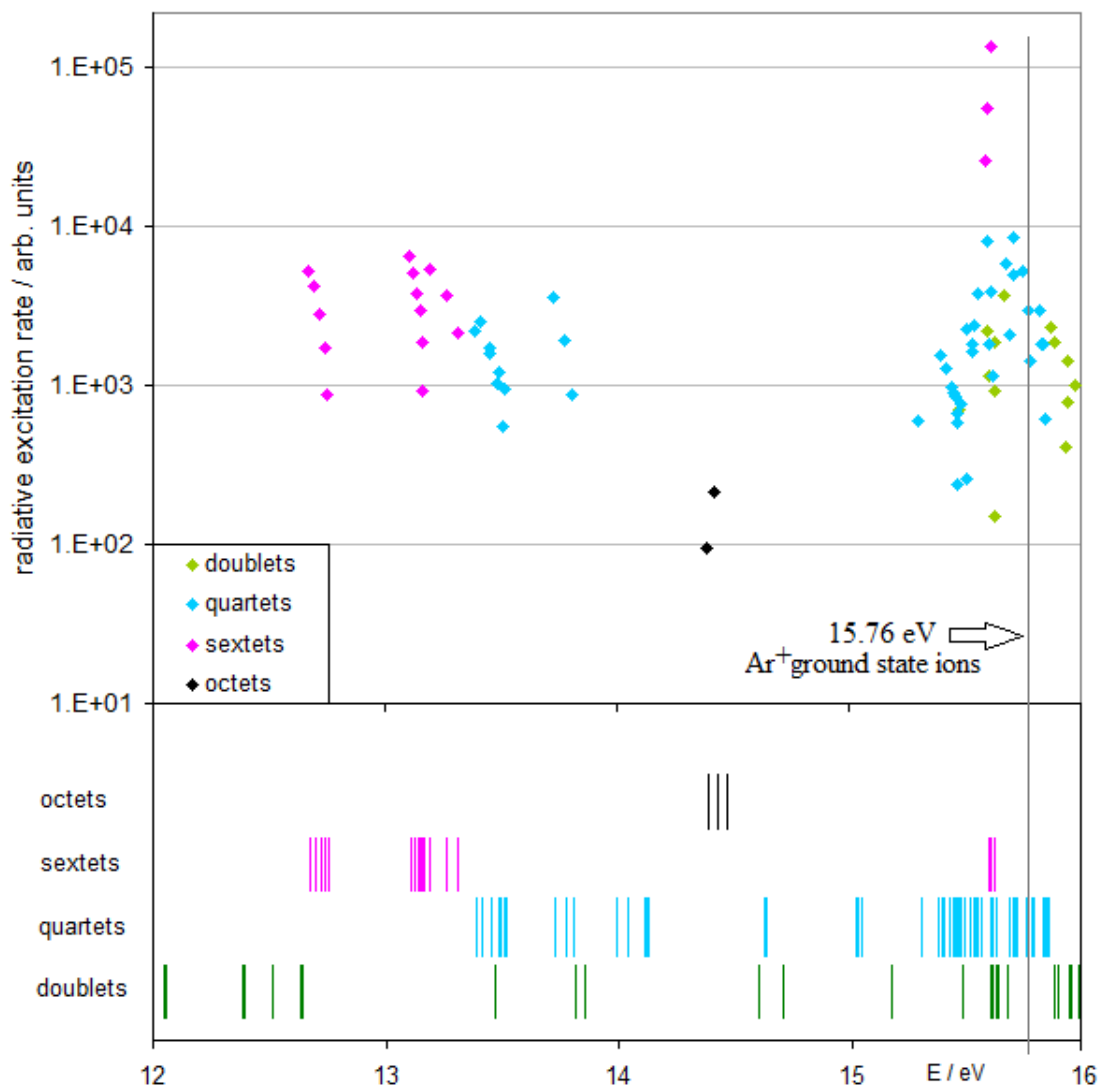


Fig. 11
 TR diagram of Fe II in an argon discharge, excitation energies 12-16 eV



1020